FGF-dependent left–right asymmetry patterning in zebrafish is mediated by Ier2 and Fibp1

Sung-Kook Hong and Igor B. Dawid[1]

Laboratory of Molecular Genetics, Eunice Kennedy Shriver National Institute of Child Health and Human Development, National Institutes of Health, Bethesda, MD, 20892

Contributed by Igor B. Dawid, December 18, 2008 (sent for review October 14, 2008)

Establishment of left–right asymmetry in vertebrates requires nodal, Wnt-PCP and FGF signaling and involves ciliogenesis in a laterality organ. Effector genes through which FGF signaling affects laterality have not been described. We isolated the zebrafish *ier2* and *fibp1* genes as FGF target genes and show that their protein products interact. Knock down of these factors interferes with establishment of organ laterality and causes defective cilia formation in Kupffer's Vesicle, the zebrafish laterality organ. Cilia are also lost after suppression of FGF8, but can be rescued by injection of *ier2* and *fibp1* mRNA. We conclude that Ier2 and Fibp1 mediate FGF signaling in ciliogenesis in Kupffer's Vesicle and in the establishment of laterality in the zebrafish embryo.

ciliogenesis | Kupffer's vesicle | laterality

While bilaterians are broadly symmetrical along the left/right (L/R) axis, substantial asymmetries exist that are an essential feature of the animal's body plan. In humans, various types of L/R defects arise, leading to abnormal positioning of organs, skeletal malformation, and failure of neural tube closure (1). Establishment of L/R asymmetry in vertebrates has been studied extensively, leading to the implication of several signaling pathways in the process (2–6). Although the nature of the initial symmetry-breaking event remains elusive, subsequent regulatory cascades have been elucidated to a considerable extent and shown to be conserved in evolution (6). Ciliogenesis in the mouse node and in equivalent structures such as zebrafish Kupffer's vesicle, chick Hensen's node, and *Xenopus* gastrocoel roof plate, is essential for the establishment of L/R asymmetry (7–12). The rotation of monocilia in these fluid-filled cavities generates leftward nodal flow, which deposits vesicles containing signaling factors on one side of the node (9), presumably leading to L/R polarization. Although an alternative model has been proposed in which cilia act as mechanosensory devices (3, 13, 14), the importance of cilia as such in laterality establishment is clear. Recently, a role for Bardet-Biedl syndrome proteins (15, 16) and for noncanonical Wnt/planar cell polarity (PCP) signaling (17) has been reported in early ciliogenesis and laterality establishment. In mice and zebrafish, these pathways are also involved in regulating cell movements in development, and interference with their function leads to midline defects in addition to laterality defects. These observations, and correlations seen in zebrafish mutants (18), point to an association of midline and laterality defects in vertebrate embryos.

Several signaling pathways have been implicated in L/R asymmetry, notably the nodal and hedgehog pathways (2–6). Fibroblast growth factor (FGF) signaling is known to have a role in this process, although opposite effects on laterality have been reported for the mouse and chick (19–21). Studies in the rabbit suggest that the differences are dominated by the geometry of the early embryo (22). In zebrafish *ace/fgf8* mutants, laterality of brain, heart, and gut is frequently abnormal, and a fraction of the mutant embryos show defects in Kupffer's vesicle (23). In the mouse, FGF signaling induces vesicular traffic that leads to the asymmetric deposition of other signaling factors at one side of the node, presumably generating nodal asymmetry that leads to a transfer of the L/R signal to the lateral plate mesoderm (9). Although this latter study indicates that FGF functions in L/R asymmetry by controlling vesicle trafficking, the effects of FGF on the expression of nodal and lefty2 suggest an additional role in transcriptional regulation. The mechanism of FGF action and possible effector molecules transmitting the signal in L/R asymmetry establishment are presently unknown.

Here, we report the isolation of *ier2* and *fibp1* as FGF target genes that cooperate in laterality determination in zebrafish. Knock down of each gene affects ciliogenesis and establishment of L/R asymmetry, and the two genes are synergistic in their function. Further, supplementation with *ier2* and *fibp1* mRNAs can rescue ciliogenesis in Kupffer's vesicle that has been impaired by depletion of FGF8. Thus, we provide evidence for the functional interaction of Ier2 and Fibp1, and for their joint requirement downstream of FGF8 for ciliogenesis in Kupffer's vesicle and for the establishment of laterality in the zebrafish embryo.

Results

Identification of Ier2 and Physical Interaction with Fibp1. We used microarray analysis to screen for effectors of FGF signaling by comparing the transcriptome of embryos injected with control, *fgf8*, or dominant negative *fgf receptor 4* (*dnfgfr4*) RNA. We first focused on one of the FGF-induced genes, *immediate early response 2* (*ier2*, also known as *pip92*), a gene activated by growth factors in cell culture whose in vivo functions have not been characterized to date (24–26). To probe Ier2 function we used it as a bait in yeast 2-hybrid screening experiments. These studies yielded *fgf intra-cellular binding protein 1*(*fibp1*) as a major interacting factor. Fibp1 is known to be a nuclear FGF binding protein, but as in the case of Ier2, its in vivo functions have not been elucidated (27, 28). Ier2 is partly and Fipb1 is highly conserved among vertebrates (Figs. S1 and S2). In the zebrafish embryo, *ier2* shows an FGF syn-expression group pattern at early stages (29, 30) and is later detected in the notochord and caudal region, whereas *fibp1* expression is ubiquitous (Figs. S3 and S4). To check the microarray results we performed in situ hybridization with *ier2* and *fibp1* after injection of *fgf8* or *dnfgfr4* RNA into zebrafish embryos. Both genes were strongly induced by *fgf8* and suppressed by *dnfgfr4* RNA (Fig. 1 *A–F*), confirming that they are downstream targets of the FGF signaling pathway. We also tested the yeast 2-hybrid results by coimmunoprecipitation experiments after cotransfection of Flag-tagged Ier2 and HA-tagged Fibp1 into cultured cells. Reciprocal tests showed effective coprecipitation of the two proteins (Fig. 1 *G* and *H*). Further, the two proteins colocalized in the nucleus after

Author contributions: S.-K.H. and I.B.D. designed research, S.-K.H. performed research; S.-K.H. and I.B.D. analyzed data, and S.-K.H. and I.B.D. wrote the paper.

The authors declare no conflict of interest.

[1]To whom correspondence should be addressed. E-mail: idawid@mail.nih.gov.

This article contains supporting information online at www.pnas.org/cgi/content/full/0812880106/DCSupplemental.

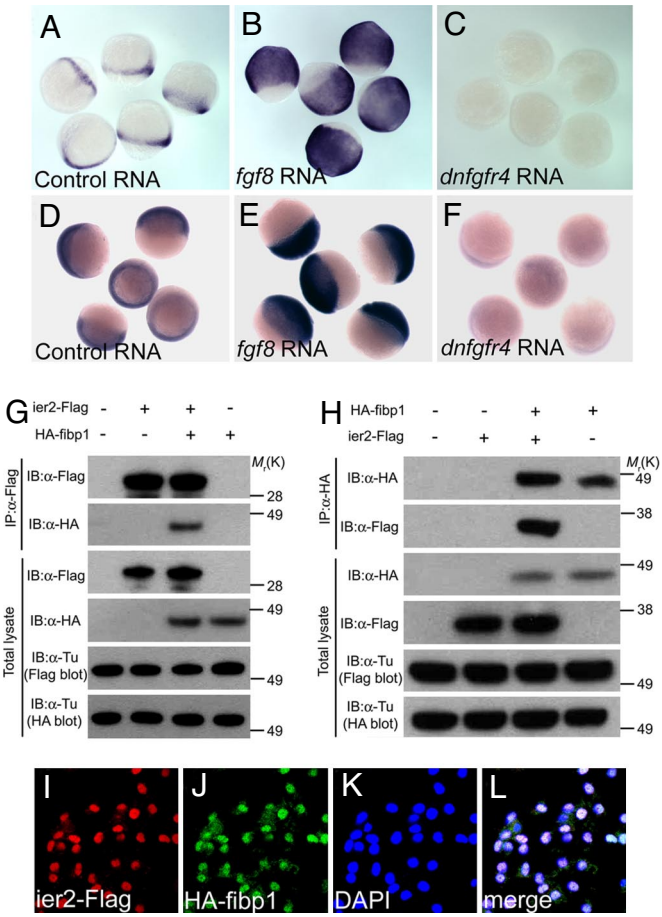

Fig. 1. Ier2 and Fibp1 are Downstream of FGF. (*A–F*) Whole-mount in situ hybridization with *ier2* (*A–C*) at 80% epiboly, and with *fibp1* (*D–F*) at 60% epiboly stages after injection of control *gfp* RNA, 100 pg (*A* and *D*); *fgf8* RNA, 5 pg (*B* and *E*); and *dnfgfr4* RNA, 300 pg (*C* and *F*). (*G* and *H*) Physical interaction between Ier2 and Fibp1. Immunoprecipitation (IP) and immunoblotting (IB) are indicated. (*I–L*) Intracellular localization of Ier2 and Fibp1. Ier2 (*I*) and Fibp1 (*J*) are colocalized in the nucleus (*K*) after injection of epitope-tagged constructs into zebrafish embryos. (*L*) Merged image *I–K*

injection of epitope-tagged RNAs into zebrafish embryos at shield and 80% epiboly stages (Fig. 1 *I–L*) and after transfection into 293T cells (data not shown). These data indicate that Ier2 and Fibp1 are FGF induced factors that can physically interact in the nucleus during embryonic development.

Phenotypes of *ier2* and *fibp1* Morphants. To investigate Ier2 and Fibp1 function, we performed knockdown experiments, using antisense morpholino oligonucleotides (MO) targeted to the translational start region of each mRNA. Both MOs are highly effective, as tested by coinjection of RNAs encoding gfp-tagged Ier2 or Fibp1 with the cognate MO into zebrafish embryos (Fig. S5). Injection of *ier2* MO into 1-cell embryos resulted in reduced expansion toward the anterior consistent with defects in cell movements (92% shortened axis, $n = 80$), compared with control MO-injected embryos (1%, $n = 87$) (Fig. 2 *A* and *C*). Likewise, convergence to the midline appeared compromised, resulting in widened notochord and somites (Fig. 2 *B*, *D*, *E–L*). At 24 h after fertilization (hpf), *ier2* MO-injected embryos had a short axis (95%, $n = 90$; control MO-injected embryos were 100% normal, $n = 89$). This phenotype was successfully rescued by zebrafish *ier2* mRNA (10% axis defects, $n = 76$), and by human *ier2* RNA (11%, $n = 65$) (Fig. 3 *A–D*). These data indicate that zebrafish and human Ier2 are functionally equivalent despite

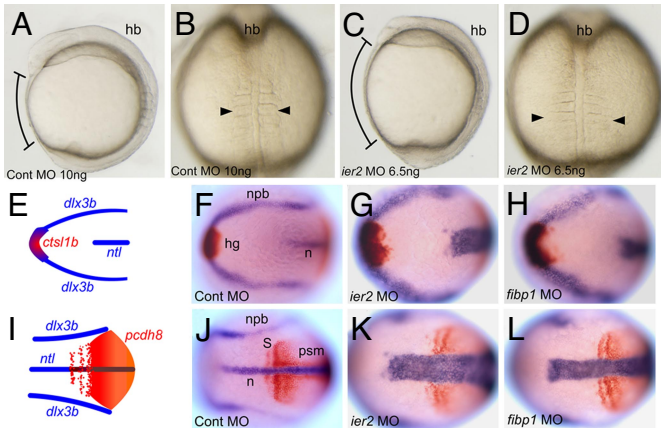

Fig. 2. Ier2 and Fibp1 are required for convergent extension. Control (*A* and *B*) and *ier2* morphant (*C* and *D*). Lateral (*A* and *C*) and dorsal (*B* and *D*) views at the 5-somite stage. Brackets in A and C show the distance between head and tail, and arrowheads in B and D show the width of the somites. (*E–L*) Two-color in situ hybridization with marker genes at the 3-somite stage. Dorsal views of anterior (*E–H*) and posterior (*I–L*) region. (*E* and *I*) Drawings of a normal embryo indicating the patterns of the markers used, *ctsl1b* (red), *dlx3b* (blue), *ntl* (blue), and *pcdh8* (red). (*F* and *J*) Control MO-injected embryo. (*G* and *K*) *ier2* MO-injected embryo. (*H* and *L*) *fibp1* MO-injected embryo. In the experimental embryos, notochord and somites are wider and extension along the A/P axis is reduced.

limited sequence conservation (Fig. S1). The MO effects are dose dependent, as shown in 48 hpf embryos (Fig. 3 *F–I*). This allowed a test for functional interaction between Ier2 and Fibp1. Low doses of individual MOs had little effect (*ier2* MO at 2 ng, 5% axis defects, $n = 71$; *fibp1* MO at 3 ng, 11%, $n = 101$; control MO, 5%, $n = 67$) (Fig. 3 *E*, *F*, and *H*). In contrast, a combination of both MOs at low dose resulted in a phenotype similar to that induced by high doses of individual MOs (both MOs at low dose, 81% axis defects, $n = 78$; *ier2* MO at 6.5 ng, 91%, $n = 71$; *fibp1* MO at 7 ng, 89%, $n = 68$; Fig. 3 *G*, *I*, and *J*). FGF signaling can dorsalize zebrafish embryos (31). Because Ier2 and Fibp1 are induced by FGF and may participate in FGF signal transduction we tested for effects of the MOs on dorsal/ventral axis specification. No changes in the pattern of expression of the ventral marker *bmp4* and the dorsal maker *chordin* were observed at early and mid gastrula stages (Fig. S6).

Overexpression of Ier2 and Fibp2 also led to shortened axis compatible with inhibition of cell movements in the embryo, as observed at the gastrula stage and at 48 hpf (Fig. S7 and Fig. 3). It is common for cell movements to be impaired by both overexpression and suppression of gene involved in the process. The overexpression phenotype also served to confirm functional interaction between the two proteins. Effective doses of individual RNAs generated similar phenotypes (*ier2* RNA at 50 pg, 95% axis defects, $n = 87$; *fibp1* RNA at 70 pg, 99%, $n = 72$; *hier2* RNA at 50 pg, 90%, $n = 74$), control RNA (2% axis defects, $n = 78$), low doses of *ier2* RNA (10%, $n = 56$) or *fibp1* RNA (7%, $n = 70$) had little effect, and coinjection of low doses showed a synergistic effect (88%, $n = 86$) (Fig. 3 *M–S*). Finally, Ier2 and Fibp1 were able to cross rescue each other: *fibp1* RNA reduced the effect of *ier2* MO to 22% axis defects ($n = 68$) as opposed to 91% for *ier2* MO alone (see above), and *ier2* RNA rescued *fibp1* MO to 18% defects ($n = 84$) as opposed to 89% for *fibp1* MO alone (Fig. 3 *K* and *L*). The cross rescue may be due to a reduction rather than complete elimination of each protein by the cognate MO; the remaining protein might then be more effectively incorporated into complexes by increased concentration of its partner. These data support the view that Ier2 and Fibp1 functionally interact in vivo.

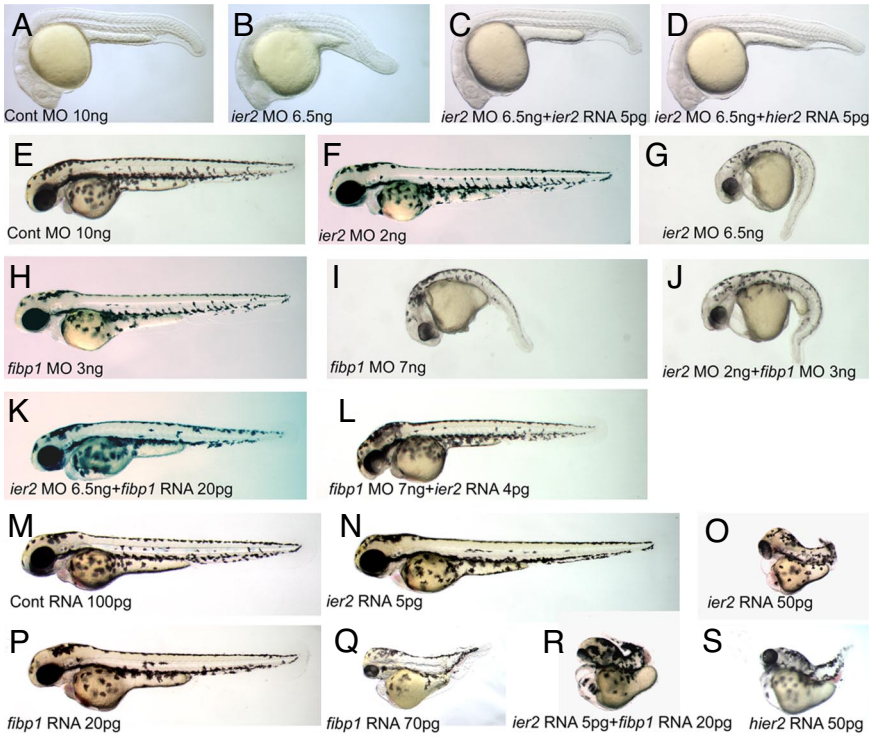

Fig. 3. Functional interaction between Ier2 and Fibp1. (*A–D*) Lateral views at 24 hpf. The *ier2* MO-injected embryo has a short trunk (*B*) compared with the control (*A*). The *ier2* MO phenotype was rescued by coinjection with zebrafish *ier2* mRNA (*C*) and human *ier2* mRNA (*D*). (*E–S*). Lateral views at 48 hpf. (*E–L*) Knock down phenotypes. Low doses of *ier2* MO (*F*) or *fibp1* MO (*H*) have no phenotype, whereas effective doses of *ier2* MO (*G*) and *fibp1* MO (*I*) show very similar phenotypes. Coinjection with both MOs at low dose mimics the high-dose phenotype (*J*). *ier2* MO is rescued by *fibp1* RNA (*K*), and *fibp1* MO is rescued by *ier2* RNA (*L*). (*M–S*) *Ier2* and *fibp1* overexpression phenotypes. (*M*) Control RNA-injected embryos. (*N* and *O*) *ier2* RNA injection phenotypes at low dose and effective dose. (*P* and *Q*) *fibp1* RNA injection phenotypes at low dose and effective dose. (*R*) Coinjection of low dose of *ier2* plus *fibp1* RNA. (*S*) Injection of human *hier2* RNA.

Failure of Organ Laterality in *ier2* and *fibp1* Morphants. Because of the association of convergent extension and laterality defects (16, 32), we investigated the establishment of L/R asymmetry in embryos injected with *ier2* or *fibp1* MO. Severe deficits in laterality were observed after injection of either MO at high dose or a combination of the two MOs at low doses (Fig. 4). The *Nodal*-related genes *southpaw* (*spaw*) (33) and *lft1* (34) are normally expressed on the left side, but embryos in which expression of Ier2, Fibp1, or both was suppressed showed reversed or bilateral expression of *spaw* (Fig. 4 *A–D* and *Q*) and *lft1* (data not shown). Because both *spaw* and *lft1* are required for establishment of laterality, any disturbance in their expression pattern is correlated with defects in organ placement in zebrafish and other organisms (33–36). We assayed for effects on heart and gut laterality in *ier2* and *fibp1* morphants, using *cmlc2* (37) and *foxa3* (38) as markers to visualize the early development of these organs. Ier2 and Fibp1 morphant embryos have extensive heart laterality and looping deficits, showing a predominance of *situs inversus* (Fig. 4 *E–H* and *Q*). Likewise, *foxa3* expression in the developing gut illustrates the frequent failure of gut looping to the left in the morphant embryos (Fig. 4 *I–L* and *Q*). As in heart development, gut looping showed a predominance of inverted phenotypes in the morphants, most notably in the *ier2*/*fibp1* double morphants (Fig. 4*Q*). It is known that reduction in *spaw* expression randomizes gut laterality (38), whereas the depletion of Ier2 and Fibp1 led to a predominance of *situs inversus* even though *spaw* was expressed bilaterally in a majority of the morphant embryos. These observations suggest that Ier2 and Fibp1 are required for the establishment of laterality of visceral organs in the zebrafish upstream of *spaw*, but that additional factors are likely to be affected.

An additional phenotype observed in the *ier2* and *fibp1* morphant embryos is undulation of the notochord, as visualized by in situ hybridization with *shh* (Fig. 4 *M–P*) and *lft1* (37) (data not shown). Establishment of laterality is often compromised in midline defect mutants in zebrafish (2, 18), and notochord undulation has been associated with laterality defects (16).

Ier2 and Fibp1 Are Required for Ciliogenesis in Kupffer's Vesicle. Kupffer's vesicle, a fluid-filled structure, is located beneath the tail bud in the zebrafish embryo and is the functional equivalent of the mammalian node (10). Kupffer's vesicle cells carry monocilia, and these cilia and possibly the fluid flow that depends on their function, are critical for the establishment of laterality in zebrafish (6, 9). It is known that *ace*/*fgf8* mutant zebrafish suffer defects in Kupffer's vesicle formation and exhibit abnormal laterality of pharyngeal arches and visceral organs (23), and L/R asymmetry phenotypes after the loss of FGF signaling have been reported in other organisms as well (9, 19, 23). We investigated the role of FGF signaling and of Ier2 and Fibp1 in the development of cilia in Kupffer's vesicle. Injection of an *fgf8* MO led to a dramatic loss of cilia in Kupffer's vesicle (87% of embryos with reduced cilia, $n = 21$) compared with control MO-injected embryos (2%, $n = 20$) (Fig. 5 *A*, *B*, and *G*). Likewise, injection of *ier2* MO (80%, $n = 23$) or *fibp1* MO (88%, $n = 20$) separately caused a partial loss of cilia (Fig. 5 *C*, *D*, and *G*), with the length of the remaining cilia reduced. The evidence for cooperation between the two factors is further supported by an almost complete loss of cilia after coinjection of *ier2* and *fibp1* MOs (90%, $n = 21$) (Fig. 5 *E* and *G*), yielding a phenotype similar to that of knockdown of FGF8 (Fig. 5 *B* and *G*). Most critically, the loss of cilia elicited by suppression of FGF8

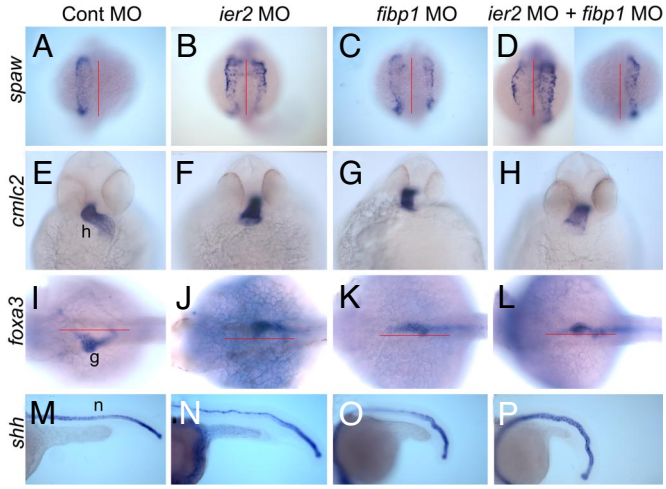

Q

	cont MO			ier2 MO			fibp1 MO			Both MO's		
	n=56			*n*=53			*n*=76			n=66		
spaw	L	R	Bi	L	R	Bi	L	R	Bi	L	R	Bi
	55	0	1	3	8	42	4	22	50	0	36	30
	n=47			*n*=55			*n*=65			*n*=45		
cmlc2	L	R	M	L	R	M	L	R	M	L	R	M
	47	0	0	3	42	10	5	40	20	0	38	7
	n=45			*n*=52			*n*=54			*n*=49		
foxa3	L	R	M	L	R	M	L	R	M	L	R	M
	42	3	0	4	38	10	2	30	22	0	43	6

Fig. 4. Ier2 and Fibp1 are required to establish left–right asymmetry in zebrafish. Control MO (*A*, *E*, *I*, and *M*), *ier2* MO, 6.5 ng (*B*, *F*, *J*, and *N*), *fibp1* MO, 7 ng (*C*, *G*, *K*, and *O*), and *ier2* MO plus *fibp1* MO, 2 plus 3 ng (*D*, *H*, *L*, and *P*) were injected, and embryos examined by whole-mount in situ hybridization. (*Q*) Quantification of experiments illustrated in A-L. (*A–D*) Dorsal view of *spaw* expression at 19 hpf. MO-injected embryos show bilateral expression (*B–D*) compared with left side expression of controls (*A*). (*E–H*) Ventral view of *cmlc2* expression at 36 hpf. *Ier2* and *fibp1* MO cause abnormal heart laterality and looping (*F–H*); control in *E*. (*I–L*) Asymmetric expression of *foxa3* in gut was altered by *ier2* or *fibp1* MO injection (*J–L*), compared with controls (*I*), all at 36 hpf. (*M–P*) *Ier2* and *fibp1* MOs caused notochord undulation at 22 hpf. h, heart; g, gut; n, notochord.

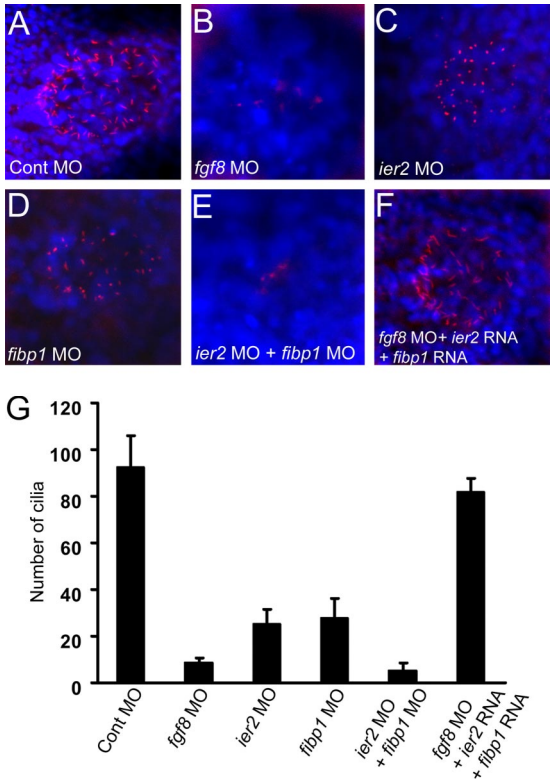

Fig. 5. Cilia formation in Kupffer's vesicle depends on Ier2 and Fibp1. (*A–F*) Monocilia were detected with anti-acetylated tubulin antibody (red), and nuclei with DAPI (blue) in Kupffer's vesicle at the 5-somite stage. *fgf8* MO, 8 ng (*B*) and *ier2* MO plus *fibp1* MO (*E*) -injected embryos show dramatic reduction of cilia, compared with control (*A*). Moderate reduction of cilia by *ier2* MO (*C*) or *fibp1* MO (*D*) alone was observed. Loss of cilia was rescued by coinjection with *ier2* RNA plus *fibp1* RNA with *fgf8* MO (*F*). For levels of MOs see legend to Fig. 4. (*G*) Number of cilia in Kupffer's vesicle; 12 embryos were counted in each case corresponding to images in (*A–F*). n, notochord.

expression was effectively reversed by coinjection of *ier2* plus *fibp1* mRNAs with the *fgf8* MO (18%, $n = 19$) (Fig. 5 *F* and *G*). These observations provide strong evidence for the view that Ier2 and Fibp1 are cooperating factors downstream of FGF signaling that are required for the formation of Kupffer's vesicle cilia in the zebrafish. This places Ier2 and Fibp1 upstream of the information transfer from the node to the lateral plate mesoderm during laterality establishment in the zebrafish embryo.

To gain more insight into the relationship between *fgf8* and *ier2* in Kupffer's vesicle formation we carried out a detailed comparison of their expression patterns in this region of the embryo. Both genes are expressed in Kupffer's vesicle and presomitic mesoderm (Fig. 6 *A* and *B*). Double label fluorescence in situ hybridization of *ier2* with *fgf8* and with *charon* (*cha*), a marker for Kupffer's vesicle, shows colocalization of *fgf8* and *ier2* in Kupffer's vesicle, with *cha* limited to a horseshoe-shaped caudal region, as reported in ref. 39 (Fig. 6 *C* and *D*). Thus, FGF8, Ier2 and Charon, together with the ubiquitously expressed Fibp1, are in a position to affect the function of Kupffer's vesicle in the specification of laterality. A relationship between these factors is further supported by the observation that injection of *fgf8* MO or a combination of *ier2* and *fibp1* MOs led to a loss of *cha* expression in Kupffer's vesicle (Fig. 6 *F* and *G*). As in the case of cilia (Fig. 5*F*), the loss of *cha* expression elicited by *fgf8* MO was rescued by coinjection of *ier2* plus *fibp1* RNA (Fig. 6*H*). Kupffer's vesicle is formed from a set of cells in the early gastrula called the forerunner cells (40). In embryos injected with *ier2* MO, *fibp1* MO or both, forerunner cells could still be detected although they were disorganized and broken up into multiple groups of cells (Fig. 6 *I–L*). Thus, Ier2 and Fibp1 appear to affect Kupffer's vesicle formation starting at the time of forerunner cell formation.

Discussion

Involvement of the FGF signaling pathway in establishment of L/R asymmetry has been reported in several organisms including the mouse, chick, rabbit, and zebrafish (9, 19–23). One study focused on the role of FGF in facilitating vesicular deposition on one side of the node (9), whereas other studies showed a requirement for FGF signaling for the expression of other genes and for the final laterality of different organs in the embryo (19–23). The mechanism of FGF function in laterality and the nature of mediators acting downstream of FGF in this process are largely unknown. In the present article, we describe the identification of the *early immediate response 2* (*ier2*) gene as an FGF target gene in the zebrafish embryo, using microarray analysis. *Ier2* was discovered as a growth-factor inducible gene (24) whose expression in cultured cells could be activated by Ets and CArG-like elements (25). The function of Ier2 in embryonic development has not been studied. Although the overall sequence similarity between the zebrafish protein and human and

DEVELOPMENTAL BIOLOGY

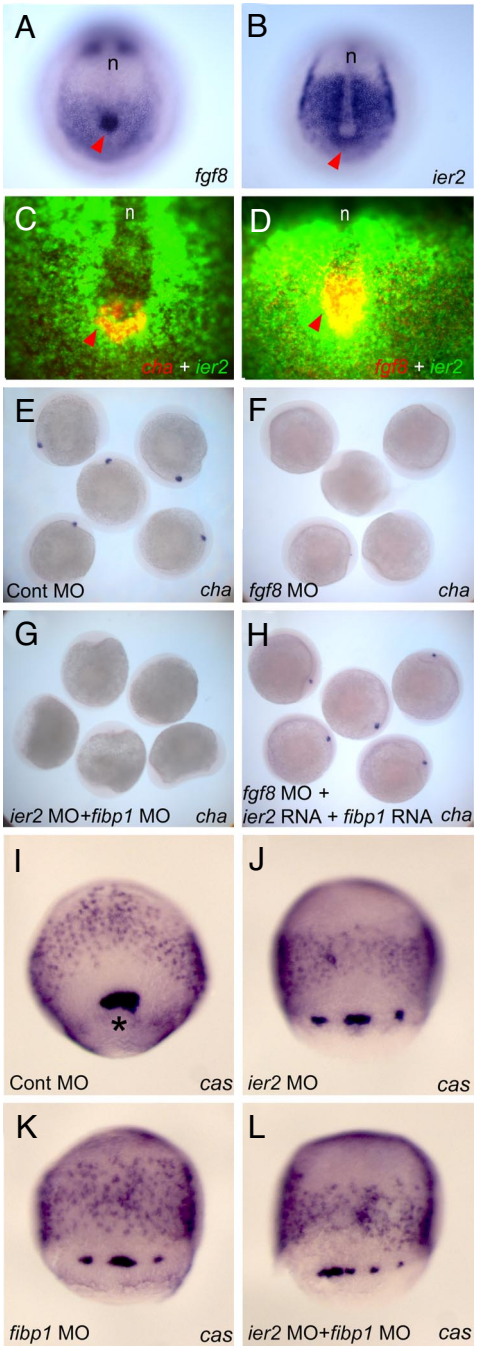

Fig. 6. Involvement of Ier2 and Fibp1 in forerunner cell formation and in *charon* expression in Kupffer's vesicle. (*A–H*), embryos were fixed at the 5-somite stage. Expression patterns of *fgf8* (*A* and *D*), *ier2* (*B–D*), and *cha* (*C*) in normal embryos. Red arrowheads indicate Kupffer's vesicle. (*A* and *B*) In situ hybridization with purple staining. (*C* and *D*) Fluorescence in situ hybridization. (*E–H*) *Charon* expression depends on FGF signaling and Ier2/Fibp1 function. Embryos were hybridized with *cha* probe after injection of control MO (*E*), *fgf8* MO (*F*), *ier2* MO plus *fibp1* MO (*G*), and *fgf8* MO + *ier2* RNA + *fibp1* RNA (*H*). (*I–L*) Embryos at 80% epiboly hybridized with *casanova* (*cas*) probe, which highlights dorsal forerunner cells labels endoderm. An asterisk points to dorsal forerunner cells. The embryos were injected with the MO indicated. For levels of MOs see legends to Fig. 4 and 5. n, notochord.

mouse Ier2 is moderate, we found that the N-terminal region and 2 additional short segments in the middle of the protein are highly conserved. Rescue of the Ier2 loss-of-function phenotype in zebrafish by injection of human *IER2* mRNA (Fig. 3*D*) supports the view that the protein we study is the ortholog of human IER2. To understand Ier2 function, we performed a yeast 2-hybrid screen, leading to the discovery of FGF intracellular binding protein 1 (Fibp1) as an Ier2-interacting partner. Both Ier2 and Fibp1 are localized in the nucleus. We confirmed the in vivo interaction between these proteins, using injection of mRNA and MO-based knockdown experiments. In both overexpression and inhibition experiments the phenotypes obtained with either factor were identical. Further, joint overexpression or inhibition acted synergistically while cross-rescue between the two proteins could be achieved. These data strongly suggest that Ier2 and Fibp1 interact functionally in the embryo. To investigate the pathway through which FGF activates *ier2* and *fibp1*, we injected mRNA encoding the FGF effector Pea3 (41), an Ets family transcription factor, into zebrafish embryos. The expression level of *ier2* and *fibp1* were dramatically increased by Pea3 overexpression (data not shown), suggesting that these two genes are downstream of the MAPK branch of the FGF pathway.

The phenotype of *ier2* or *fibp1* MO-mediated knockdown includes apparent defects in convergent extension cell movements during gastrulation. At 24 hpf, reduced notochord development is apparent by direct inspection and by in situ hybridization with *shh*; such a phenotype has been observed after interference with convergent extension, and has been linked to effects on laterality in the zebrafish embryo (16). We found that knockdown of *ier2* and *fibp1* resulted in severe L/R defects, observable by the reversion and randomization of markers of laterality such as *spaw* and *lfty2*, and by the development of internal organs at later stages (Fig. 4). These defects were traced back to a deficit of ciliogenesis in Kupffer's vesicle; cilia in this fluid filled cavity are required for the establishment of laterality in zebrafish as in the homologous organs of other vertebrates (2–7, 9, 10, 15, 16). These experiments further supported the cooperation between Ier2 and Fibp1 and the role of FGF signaling in the pathway. It is known that ciliogenesis in Kupffer's vesicle is impaired in the *ace/fgf8* mutant (23). We reproduced this effect with the aid of an FGF8 MO and showed that knockdown of Ier2 and Fibp1 phenocopies loss of FGF8 in this system. Either of these interventions also led to a loss of *cha* expression, providing an additional link to the establishment of laterality (39). Most critically, the effect of FGF8 knockdown on ciliogenesis and *cha* expression could be rescued by supplying Ier2 and Fibp1, indicating that FGF8 action in laterality establishment is mediated by these two factors.

Recently, a modulator of Nodal signaling, *Ttrap* (32), and a mediator of Wnt signaling, *duboraya* (16), were shown to be involved in the establishment of laterality. Their loss-of-function phenotypes are similar to those of *ier2* and *fibp1*, affecting cell movements and causing notochord undulation; in addition, *duboraya* is required for ciliogenesis in Kupffer's vesicle. The relationship between convergent extension movements and ciliogenesis is also implied by studies on the Bardet-Biedl Syndrome (BBS), which causes neural tube defects because of impaired Wnt-PCP signaling and ciliary dysfunction (17). The establishment of the L/R axis requires the coordinated action of multiple signaling pathways, with the nodal and hedgehog pathways most extensively studied. With the recent indication of an involvement of Wnt signaling (16) and our evidence for the role of Ier2 and Fibp1 downstream of FGF signaling, the multiple inputs in the regulation of laterality are becoming more clearly defined.

Materials and Methods

Zebrafish Strains. We used AB* line as a wild type, and mutants lines *ace*^{ti282a} and *clo*^{m378}.

In Situ Hybridization and Immunostaining. Whole-mount in situ hybridization with alkaline phosphatase-based single- or double-color reaction is described

in ref. 42. Fluorescent in situ hybridization (FISH) was performed as reported in ref. 43. Detection of tubulin in Kupffer's vesicle was performed immunostaining with anti-acetylated tubulin antibody (Sigma), and detected with Alexa Fluor 568 (Molecular Probes). DAPI was used to stain nuclei.

Microinjection of mRNA and Morpholinos. One-cell stage embryos were used for microinjection with mRNA and morpholino (MO). *Fgf8* constructs are described in ref. 30, and *dominant negative fgfr4* (*dnfgfr4*) was constructed by deletion of the intracellular domain of zebrafish *fgfr4*, and tested by its effects on several markers. *Ier2* and *fibp1* were amplified form cDNA libraries [a HeLa cell library was a gift from M. K Jang (National Institutes of Health, MD]. All injection constructs were subcloned into pCS2+ vector, and mRNA was generated using the mMESSAGEmMACHINE kit (Ambion). Morpholino antisense oligonucleotide (MO) for *ier2*, 5′-GCCTCTGCTGTGACATC**CAT**T-GTTC-3′, for *fibp1*, 5′-CCCCACAAACACATCCAACTC**CAT**G-3′were designed and purchased from Gene-Tools; the bold sequence CAT corresponds to the start codon. *Fgf8* MO is described in ref. 44; it was injected at a level of 8 ng to observe the laterality phenotype. Cellular localization of Ier2 and Fibp1 was analyzed using a Zeiss LSM510 confocal microscope after injection of *ier2-Flag* and *HA-fibp1* RNA.

Yeast 2-Hybrid, Cell Culture, and Immunoprecipitation. We constructed a yeast 2-hybrid library using the MATCHMAKER library Constructing and Screening kit (Clontech) with mRNA from 24 hpf zebrafish embryos. For transfection we used 293T cells and FuGENE 6 transfection reagent (Roche). Antibodies for immunoprecipitation (IP) and immunoblotting (IB) were anti-Flag(M2) (from mouse), anti-HA (from rabbit), and anti-acetylated tubulin (from mouse) purchased form Sigma. Proteins were detected by enhanced chemiluminescence (Western blot Dura; Pierce).

ACKNOWLEDGMENTS. We thank J.M. Gonzales for fish care, M. Tsang for sharing clones, and K. Tanegashima and H. Zhao for help in microarray experiment. This work was supported by the Intramural Research Program of the National Institute of Child Health and Human Development, National Institutes of Health.

1. Bisgrove BW, Morelli SH, Yost HJ (2003) Genetics of human laterality disorders: Insights from vertebrate model systems. *Annu Rev Genomics Hum Genet* 4:1–32.
2. Hamada H, Meno C, Watanabe D, Saijoh Y (2002) Establishment of vertebrate left–right asymmetry. *Nat Rev Genet* 3:103–113.
3. Raya A, Belmonte JC (2006) Left-right asymmetry in the vertebrate embryo: From early information to higher-level integration. *Nat Rev Genet* 7:283–293.
4. Capdevila J, *et al.* (2000) Mechanisms of left–right determination in vertebrates. *Cell* 101:9–21.
5. Speder P, Petzoldt A, Suzanne M, Noselli S (2007) Strategies to establish left/right asymmetry in vertebrates and invertebrates. *Curr Opin Genet Dev* 17:351–358.
6. Raya A, Izpisúa Belmonte JC (2008) Insights into the establishment of left–right asymmetries in vertebrates. *Birth Defects Res C Embryo Today* 84:81–94.
7. Hirokawa N, Tanaka Y, Okada Y, Takeda S (2006) Nodal flow and the generation of left–right asymmetry. *Cell* 125:33–45.
8. Nonaka S, *et al.* (1998) Randomization of left–right asymmetry due to loss of nodal cilia generating leftward flow of extraembryonic fluid in mice lacking KIF3B motor protein. *Cell* 95:829–837.
9. Tanaka Y, Okada Y, Hirokawa N (2005) FGF-induced vesicular release of Sonic hedgehog and retinoic acid in leftward nodal flow is critical for left–right determination. *Nature* 435:172–177.
10. Essner JJ, *et al.* (2005) Kupffer's vesicle is a ciliated organ of asymmetry in the zebrafish embryo that initiates left–right development of the brain, heart and gut. *Development* 132:1247–1260.
11. Kramer-Zucker AG, Wiessner S, Jensen AM, Drummond IA (2005) Organization of the pronephric filtration apparatus in zebrafish requires Nephrin, Podocin and the FERM domain protein Mosaic eyes. *Dev Biol* 285:316–329.
12. Schweickert A, *et al.* (2007) Cilia-driven leftward flow determines laterality in Xenopus. *Curr Biol* 17:60–66.
13. Levin M (2003) Motor protein control of ion flux is an early step in embryonic left–right asymmetry. *Bioessays* 25:1002–1010.
14. Tabin CJ, Vogan KJ (2003) A two-cilia model for vertebrate left–right axis specification. *Genes Dev* 17:1–6.
15. Leitch CC, *et al.* (2008) Hypomorphic mutations in syndromic encephalocele genes are associated with Bardet-Biedl syndrome. *Nat Genet* 40:443–448.
16. Oishi I, *et al.* (2006) Regulation of primary cilia formation and left–right patterning in zebrafish by a noncanonical Wnt signaling mediator, duboraya. *Nat Genet* 38:1316–1322.
17. Ross AJ, *et al.* (2005) Disruption of Bardet-Biedl syndrome ciliary proteins perturbs planar cell polarity in vertebrates. *Nat Genet* 37:1135–1140.
18. Brand M, *et al.* (1996) Mutations affecting development of the midline and general body shape during zebrafish embryogenesis. *Development* 123:129–142.
19. Ohuchi H, Kimura S, Watamoto M, Itoh N (2000) Involvement of fibroblast growth factor (FGF)18-FGF8 signaling in specification of left–right asymmetry and brain and limb development of the chick embryo. *Mech Dev* 95:55–66.
20. Boettger T, Wittler L, Kessel M (1999) FGF8 functions in the specification of the right body side of the chick. *Curr Biol* 9:277–280.
21. Meyers EN, Martin GR (1999) Differences in left–right axis pathways in mouse and chick: Functions of FGF8 and SHH. *Science* 285:403–406.
22. Fischer A, Viebahn C, Blum M (2002) FGF8 acts as a right determinant during establishment of the left–right axis in the rabbit. *Curr Biol* 12:1807–1816.
23. Albertson RC, Yelick PC (2005) Roles for fgf8 signaling in left–right patterning of the visceral organs and craniofacial skeleton. *Dev Biol* 283:310–321.
24. Charles CH, Simske JS, O'Brien TP, Lau LF (1990) Pip92: A short-lived, growth factor-inducible protein in BALB/c 3T3 and PC12 cells. *Mol Cell Biol* 10:6769–6774.
25. Latinkic BV, Lau LF (1994) Transcriptional activation of the immediate early gene pip92 by serum growth factors requires both Ets and CArG-like elements. *J Biol Chem* 269:23163–23170.
26. Schneider A, *et al.* (2004) Restriction-mediated differential display (RMDD) identifies pip92 as a pro-apoptotic gene product induced during focal cerebral ischemia. *J Cereb Blood Flow Metab* 24:224–236.
27. Kolpakova E, *et al.* (1998) Cloning of an intracellular protein that binds selectively to mitogenic acidic fibroblast growth factor. *Biochem J* 336:213–222.
28. Kolpakova E, Frengen E, Stokke T, Olsnes S (2000) Organization, chromosomal localization and promoter analysis of the gene encoding human acidic fibroblast growth factor intracellular binding protein. *Biochem J* 352:629–635.
29. Tsang M, Friesel R, Kudoh T, Dawid IB (2002) Identification of Sef, a novel modulator of FGF signalling. *Nat Cell Biol* 4:165–169.
30. Tsang M, *et al.* (2004) A role for MKP3 in axial patterning of the zebrafish embryo. *Development* 131:2769–2779.
31. Fürthauer M, Thisse C, Thisse B (1997) A role for FGF-8 in the dorsoventral patterning of the zebrafish gastrula. *Development* 124:4253–4264.
32. Esguerra CV, *et al.* (2007) Ttrap is an essential modulator of Smad3-dependent Nodal signaling during zebrafish gastrulation and left–right axis determination. *Development* 134:4381–4393.
33. Long S, Ahmad N, Rebagliati M (2003) The zebrafish nodal-related gene southpaw is required for visceral and diencephalic left–right asymmetry. *Development* 130:2303–2316.
34. Bisgrove BW, Essner JJ, Yost HJ (1999) Regulation of midline development by antagonism of lefty and nodal signaling. *Development* 126:3253–3262.
35. Bisgrove BW, Essner JJ, Yost HJ (2000) Multiple pathways in the midline regulate concordant brain, heart and gut left–right asymmetry. *Development* 127:3567–3579.
36. Ramsdell AF (2005) Left-right asymmetry and congenital cardiac defects: Getting to the heart of the matter in vertebrate left–right axis determination. *Dev Biol* 288:1–20.
37. Rohr S, Otten C, Abdelilah-Seyfried S (2008) Asymmetric involution of the myocardial field drives heart tube formation in zebrafish. *Circ Res* 102:e12–9.
38. Horne-Badovinac S, Rebagliati M, Stainier DY (2003) A cellular framework for gut-looping morphogenesis in zebrafish. *Science* 302:662–665.
39. Hashimoto H, *et al.* (2004) The Cerberus/Dan-family protein Charon is a negative regulator of Nodal signaling during left–right patterning in zebrafish. *Development* 131:1741–1753.
40. Melby AE, Warga RM, Kimmel CB (1996) Specification of cell fates at the dorsal margin of the zebrafish gastrula. *Development* 122:2225–2237.
41. Roehl H, Nüsslein-Volhard C (2001) Zebrafish pea3 and erm are general targets of FGF8 signaling. *Curr Biol* 11:503–507.
42. Hong SK, *et al.* (2005) The zebrafish kohtalo/trap230 gene is required for the development of the brain, neural crest, and pronephric kidney. *Proc Natl Acad Sci* 102:18473–18478.
43. Kosman D, *et al.* (2004) Multiplex detection of RNA expression in Drosophila embryos. *Science* 305:846.
44. Draper BW, Morcos PA, Kimmel CB (2001) Inhibition of zebrafish fgf8 pre-mRNA splicing with morpholino oligos: A quantifiable method for gene knockdown. *Genesis* 30:154–156.